



兰州大学
LANZHOU UNIVERSITY

The 7th International Workshop on DRHBc Mass Table
1-4 July 2024
Gangneung Green City, Gangneung-si, Korea.

Finite-Amplitude Method for Charge-Exchange Transitions in Axially Deformed Nuclei based on Relativistic Energy Density Functional Theory

Chen Chen

Supervisor: Prof. Yifei Niu

School of Nuclear Science and Technology
Lanzhou University

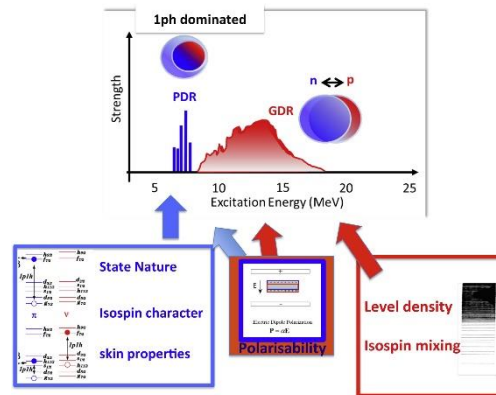
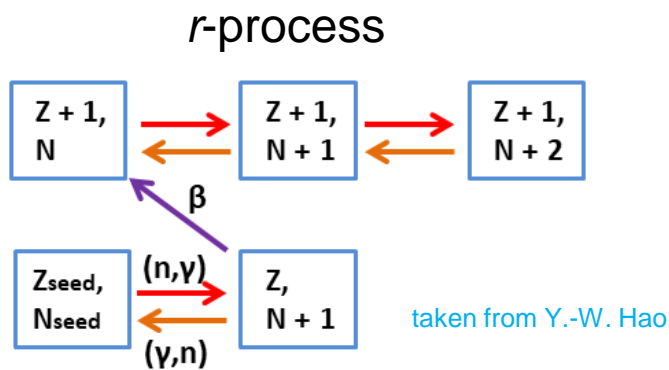
7/16/2024

- Introduction
- Theoretical Framework
- Numerical Details
- Preliminary Results
- Summary and Outlook

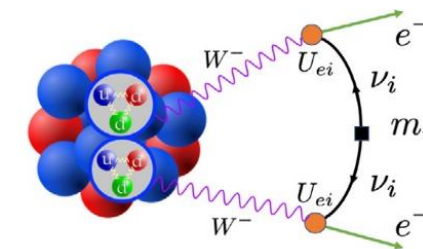
Introduction

- **Collective vibrations** are one of the hot topics in nuclear physics and astrophysics.
 - **Charge-exchange** modes: Isobaric Analog Resonance (IAR), Gamow-Teller Resonances (GTR)
 - β -decay rates in r -process
[T. Kajino et al. Prog. Part. Nucl. Phys. 107, 109 \(2019\).](#)
 - nuclear matrix elements of the neutrinoless double β -decay
[J. M. Yao et al. Prog. Part. Nucl. Phys. 126, 103965 \(2022\).](#)
 - **Non-charge-exchange** modes: Giant Dipole Resonances (GDR), Pygmy Dipole Resonances (PDR)
 - neutron capture rates in r -process
 - neutron skin thickness & symmetry energy parameters
[X. Roca-Maza et al. Prog. Part. Nucl. Phys. 101, 96 \(2018\).](#)

It's important to improve the understanding of collective vibrations!



[A. Bracco et al. Prog. Part. Nucl. Phys. 106, 360 \(2019\).](#)



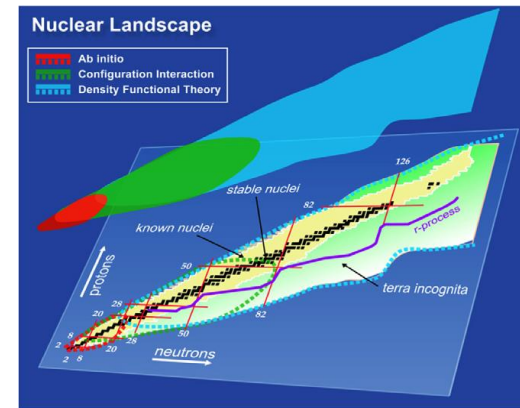
[J. M. Yao et al. Prog. Part. Nucl. Phys. 126, 103965 \(2022\).](#)

Introduction

➤ Theoretical descriptions:

- *ab initio* approach
J. Birkhan et al. Phys. Rev. Lett. 118, 252501 (2017).
- shell model
E. Caurier et al. Rev. Mod. Phys. 77, 427 (2005).
- quasiparticle random-phase approximation (QRPA)
based on density functional theory (DFT);
N. Paar et al. Rep. Prog. Phys. 70, 691–793 (2007).

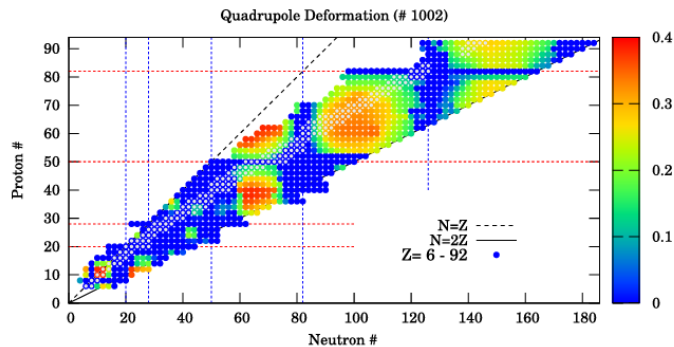
QRPA is the **most efficient** method for global descriptions,
but most applications are under **spherical approximation**.



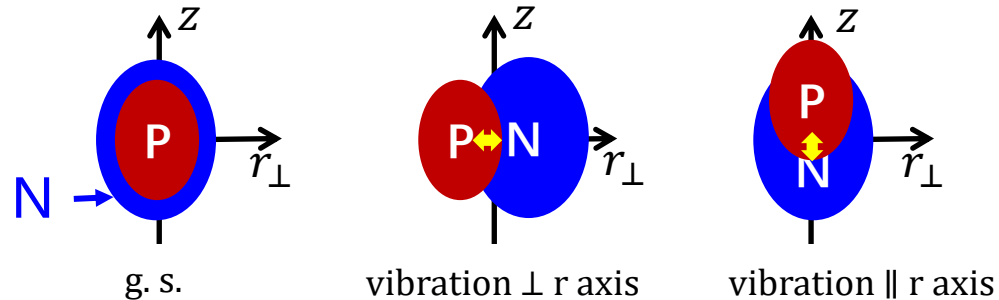
R. J. Furnstahl et al. Rep. Prog. Phys. 76, 126301 (2013).

➤ The **deformation** is necessary for global descriptions.

- Many nuclei are deformed;
- Nuclear **deformation** leads to **considerable splitting** in the transition strength.



S. Ebata et al. Phys. Scr. 92, 064005 (2017).



➤ QRPA for deformed nuclei:

- Matrix diagonalization:

[D. Pena Arteaga et al. Phys. Rev. C 77, 034317 \(2008\);](#)

[M. T. Mustonen et al. Phys. Rev. C 87, 064302 \(2013\);](#)

Experimental data are **well-reproduced**,
but the **cost** of diagonalization **increases extremely**.

- Quasiparticle finite amplitude method (QFAM):

[T. Nakatsukasa et al. Phys. Rev. C 76, 024318 \(2007\)](#)

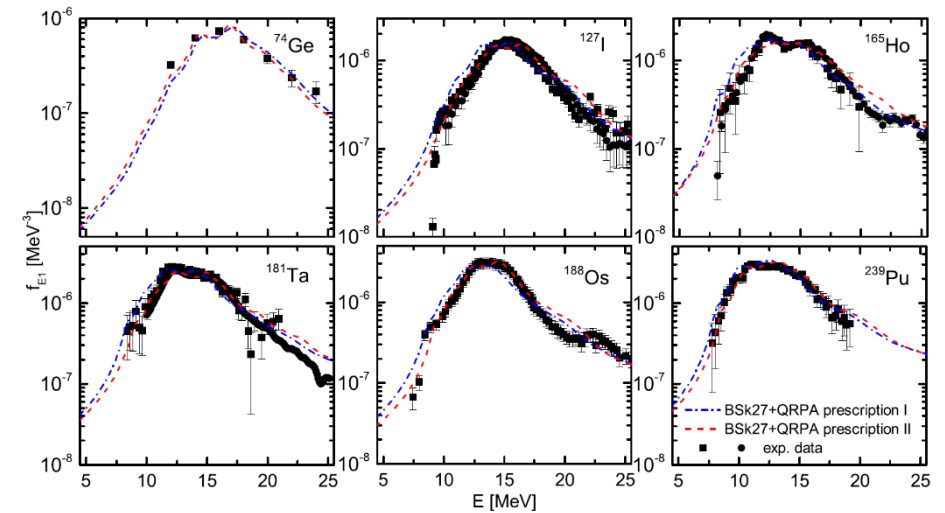
[T. Nikšić et al. Phys. Rev. C 88, 044327 \(2013\).](#)

[X. W. Sun et al. Phys. Rev. C 96, 024614 \(2017\).](#)

[A. Bjelčić et al. Comput. Phys. Commun. 253, 107184 \(2020\).](#)

Theoretically equivalent to Matrix-QRPA;

By avoiding the diagonalization routine, it's more **efficient** for global descriptions.



[Y. Xu et al. Phys. Rev. C 104, 044301 \(2021\).](#)

➤ QFAM developments:

- For non-charge-exchange transitions

Skyrme QFAM: [P. Avogadro et al. Phys. Rev. C 84, 014314 \(2011\)](#)

Relativistic QFAM: [T. Nikšić et al. Phys. Rev. C 88, 044327 \(2013\)](#), [X. W. Sun et al. Phys. Rev. C 96, 024614 \(2017\)](#)

- For charge-exchange transitions

Skyrme QFAM: [M. T. Mustonen et al. Phys. Rev. C 10 \(2016\).....](#)

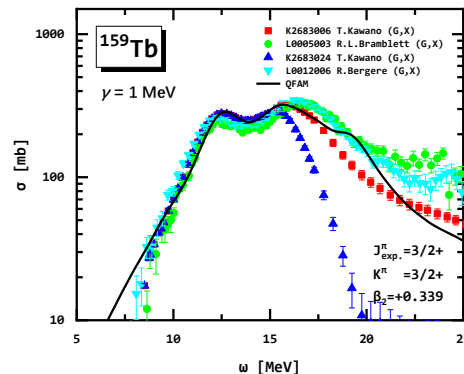
No relativistic QFAM model for charge-exchange transitions.

Although, very recently, a new method adopting liner response theory in terms of separable interactions based on relativistic DFT with speed comparable to QFAM has been introduced. [A. Ravlić et al. Preprint at <http://arxiv.org/abs/2404.13266> \(2024\).](#)

➤ Relativistic DFTs preserve the Lorentz invariance and naturally include the spin-orbit interaction.

[J. Meng et al. Prog. Part. Nucl. Phys. 57, 470 \(2006\).](#)

- Based on relativistic QFAM, we have investigated the photon-absorption cross section systemically.



In this work, our aim is to develop a relativistic QFAM model for charge-exchange transitions

Theoretical Framework

- Starting from **time-dependent Hartree-Fock-Bogoliubov equation** under the perturbation $\mathcal{F}(t)$,

$$i\hbar\partial_t\mathcal{R}(t) = [\mathcal{H}(t) + \mathcal{F}(t), \mathcal{R}(t)],$$

- The **first-order** terms above correspond to the **time-dependent linear-response equation**,

$$i\hbar\partial_t\delta\mathcal{R}(t) = [\mathcal{H}_0, \delta\mathcal{R}(t)] + [\delta\mathcal{H}(t), \mathcal{R}_0] + [\mathcal{F}(t), \mathcal{R}_0],$$

- By **Fourier** transformation, linear-response equation can be written in the **frequency** domain,

$$\omega\delta\mathcal{R}(\omega) = [\mathcal{H}_0, \delta\mathcal{R}(\omega)] + [\delta\mathcal{H}(\omega), \mathcal{R}_0] + [\mathcal{F}(\omega), \mathcal{R}_0],$$

Or written in **quasiparticle** representation ($\delta\mathcal{R}$ is represented as \mathcal{X} and \mathcal{Y}), know as **QFAM** equation,

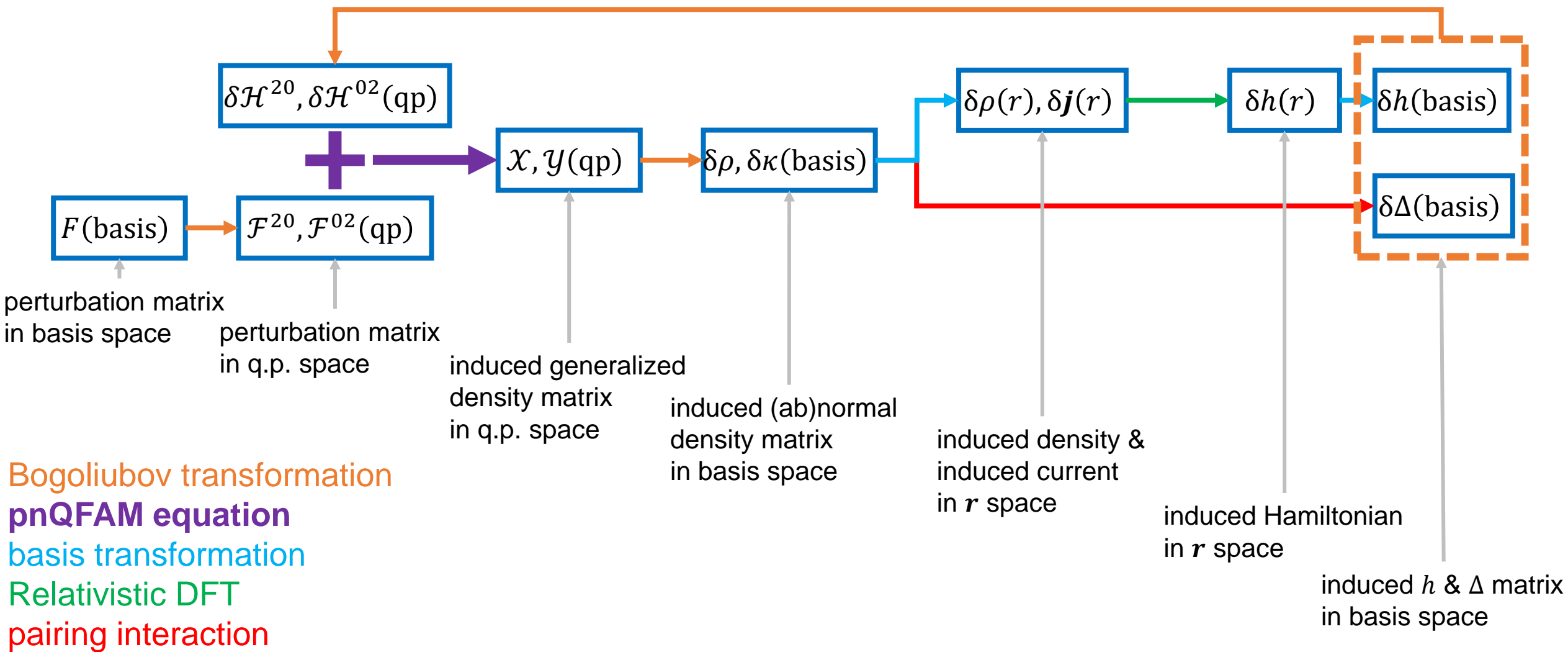
$$(E_\mu + E_\nu - \omega)\mathcal{X}_{\mu\nu}(\omega) + \delta\mathcal{H}_{\mu\nu}^{20}(\omega) = -\mathcal{F}_{\mu\nu}^{20},$$

$$(E_\mu + E_\nu + \omega)\mathcal{Y}_{\mu\nu}(\omega) + \delta\mathcal{H}_{\mu\nu}^{02}(\omega) = -\mathcal{F}_{\mu\nu}^{02},$$

For **charge-exchange** transitions, index μ & ν indicate quasiparticle with **different projected isospin**.

Theoretical Framework

➤ The flow chart of QFAM equation



➤ p-h interaction: **density-dependent point-coupling** density functional

- DD-PC1 + isovector-**pseudovector** channel $\alpha_{\text{TPV}} = 0.734$;

T. Nikšić et al. Phys. Rev. C 78, 034318 (2008); D. Vale et al. Phys. Rev. C 103, 064307 (2021).

➤ p-p interaction: finite range separable pairing interaction (included in RHB, **not yet in QFAM**)

- $G = 728 \text{ MeVfm}^3$, $a = 0.644 \text{ fm}$

Y. Tian et al. Phys. Lett. B 676, 44 (2009).

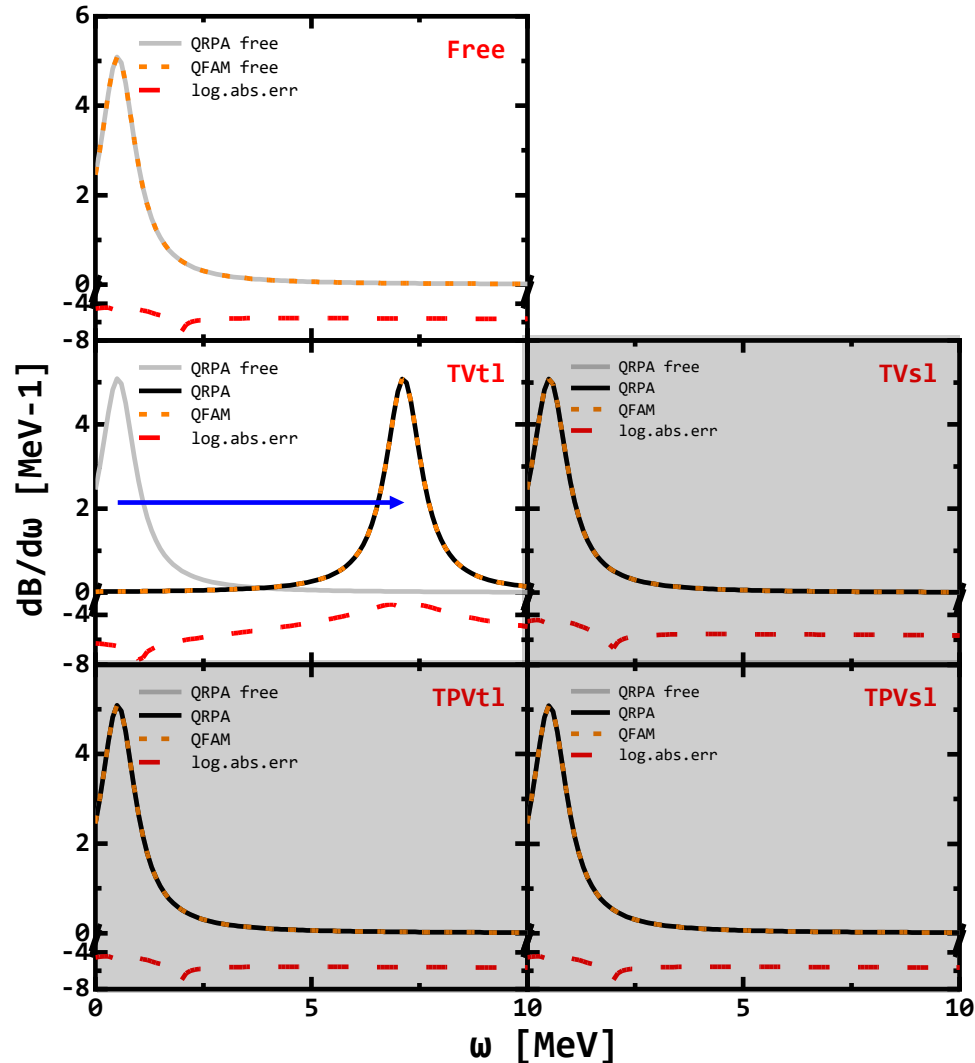
➤ Basis expansion: axially deformed harmonic oscillator (**ADHO**) basis

- RHB: only $\Omega > 0$;

- QFAM: $\Omega > 0$ & its **time-reversed** state $\bar{\Omega}$;

- Major shell quantum number truncation: $N_{\text{max}} = 14$ for large components, $N_{\text{max}} + 1$ for small components.

➤ Compared with QRPA under the **spherical** approximation: ^{48}Ca



● Fermi transition (natural parity, $J^\pi = 0^+$, $K = 0$):

- Contributions of each channel:

	isovector-vector (TV)	isovector-pseudovector (TPV)
time-like (tl)	TVtl ✓	TPVtl ✗
space-like (sl)	TVsl ✗	TPVsl ✗

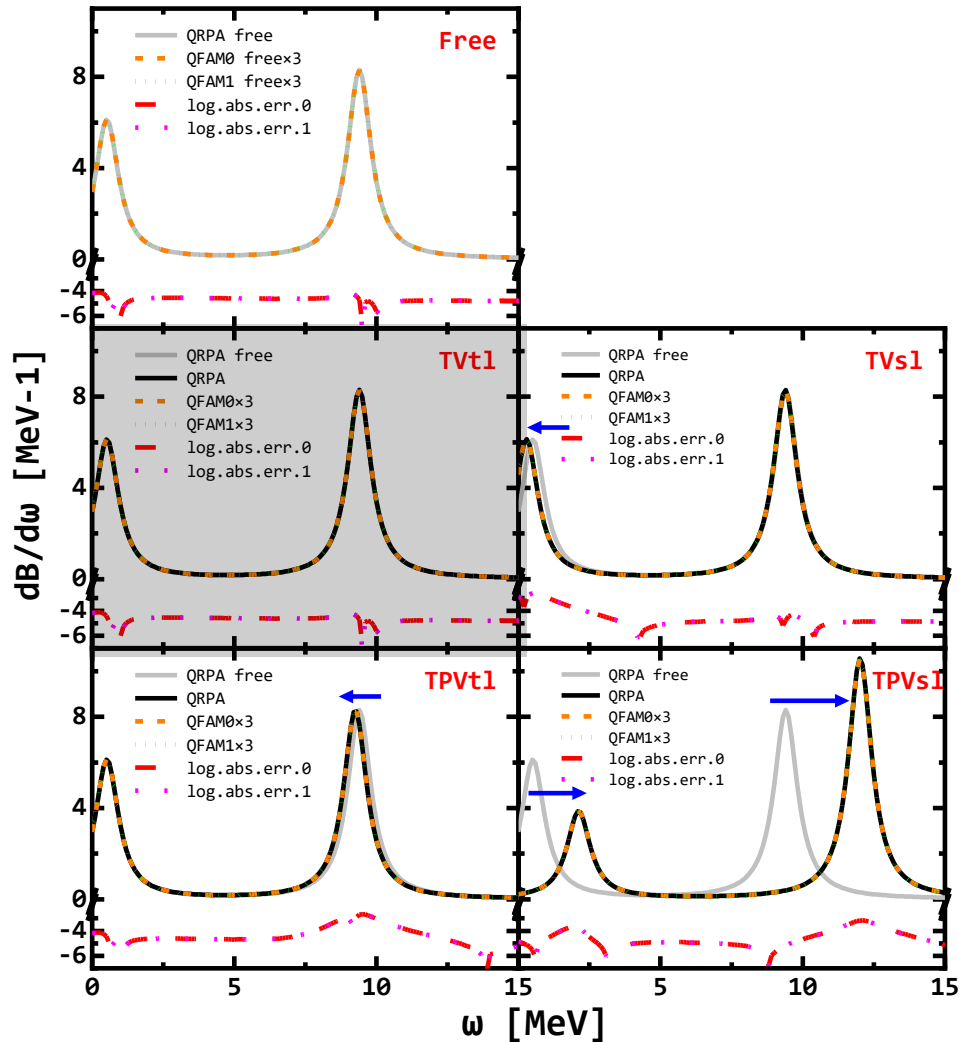
only the **TVtl** part **contributes**;

- The **numerical results** are **consistent** with above analysis;

* numerical check are truncated by $N_{\max} = 4$ for the calculation convenience.

Numerical Details

➤ Compared with QRPA under the **spherical** approximation: ^{48}Ca



● Gamow-Teller transition (Non-natural parity, $J^\pi = 1^+, K = 0, 1$):

- Contributions of each channel:

	isovector-vector (TV)	isovector-pseudovector (TPV)
time-like (tl)	TVtl ✗	TPVtl ✓
space-like (sl)	TVsl ✓	TPVsl ✓

TVsl, TPVtl & TPVsl parts contribute;

- The numerical results are consistent with above analysis;

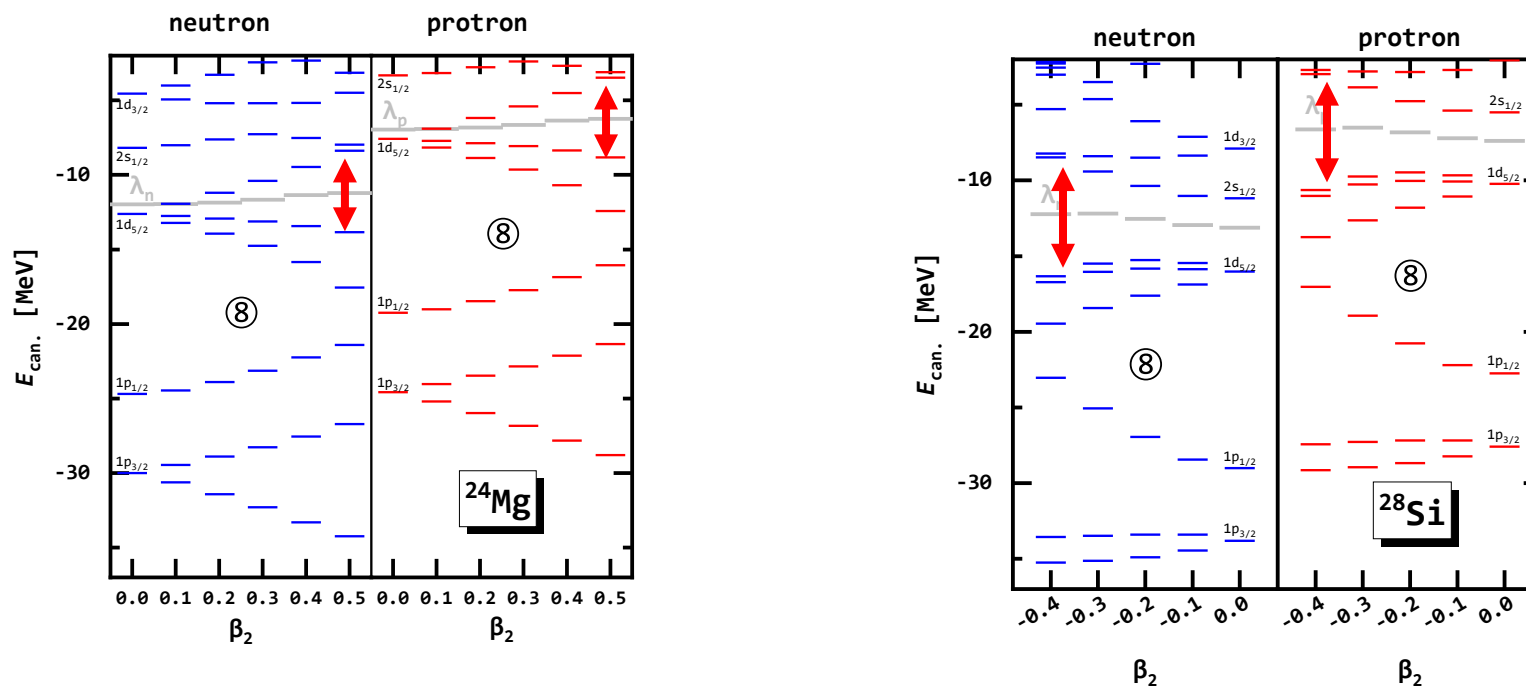
* numerical check are truncated by $N_{\max} = 4$ for the calculation convenience.

Preliminary results: Gamow-Teller Transition in ^{24}Mg & ^{28}Si

➤ Selected nuclides to illustrate the deformation effects:

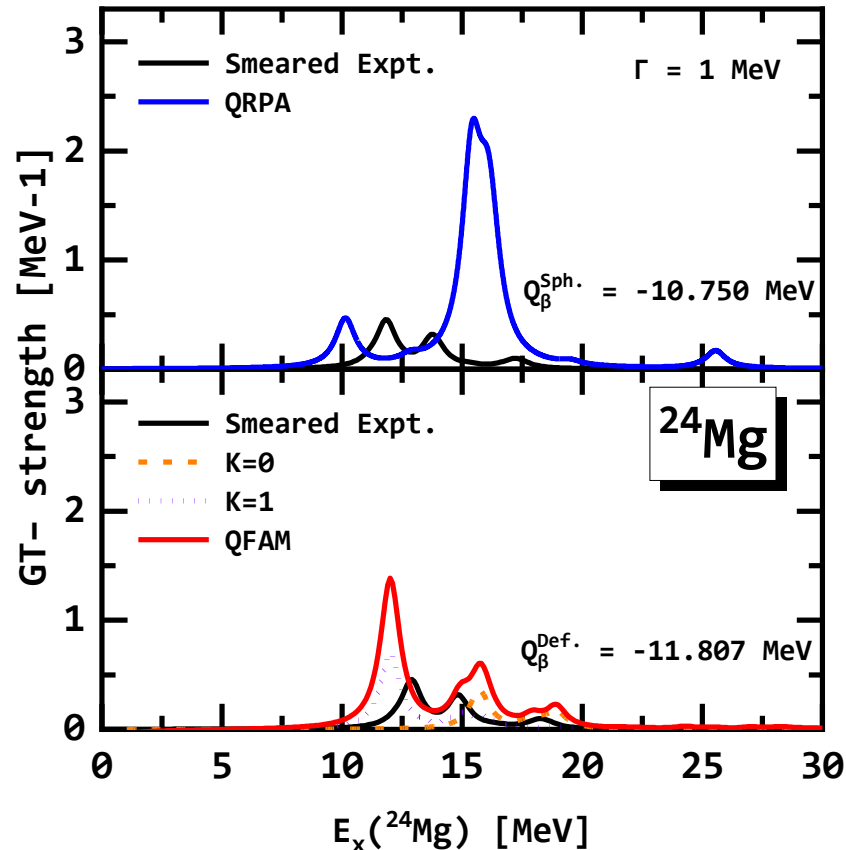
Nuclide	B. E. [MeV]	Theor.		Expt. from NNDC	
		β_2	E_{pairing} [MeV]	β_2	Pairing Gap
^{24}Mg	-194.229	+0.526	0.000	0.606	4.600
^{28}Si	-232.233	-0.376	0.000	0.412	4.353

- Considerable gaps in the well-deformed region lead to negligible pairing effects.



Preliminary results: Gamow-Teller Transition in ^{24}Mg & ^{28}Si

➤ GT- strengths of ^{24}Mg



* $^{24}\text{Mg}(^3\text{He},t)$ from R. G. T. Zegers et al. Phys. Rev. C 78, 014314 (2008).

** Expt. data shift by Q_β to compare with strength related to $E_x(^{24}\text{Mg})$

*** $Q_\beta^{\text{Def.}}$ given by deformed g.s., while $Q_\beta^{\text{Sph.}}$ given by spherical g.s..

- GTR centroid energy: $E_{\text{GTR}} = \frac{\int E_X S dE_X}{\int S dE_X}$,

Z. M. Niu. PhD thesis (2011).

	$E_{\text{GTR}}^{\text{Expt.}}$ [MeV]	$E_{\text{GTR}}^{\text{Theor.}}$ [MeV]	$E_{\text{GTR}}^{\text{Theor.}} - E_{\text{GTR}}^{\text{Expt.}}$ [MeV]
Sph.	13.257	15.137	+1.880
Def.	14.275	14.103	-0.172

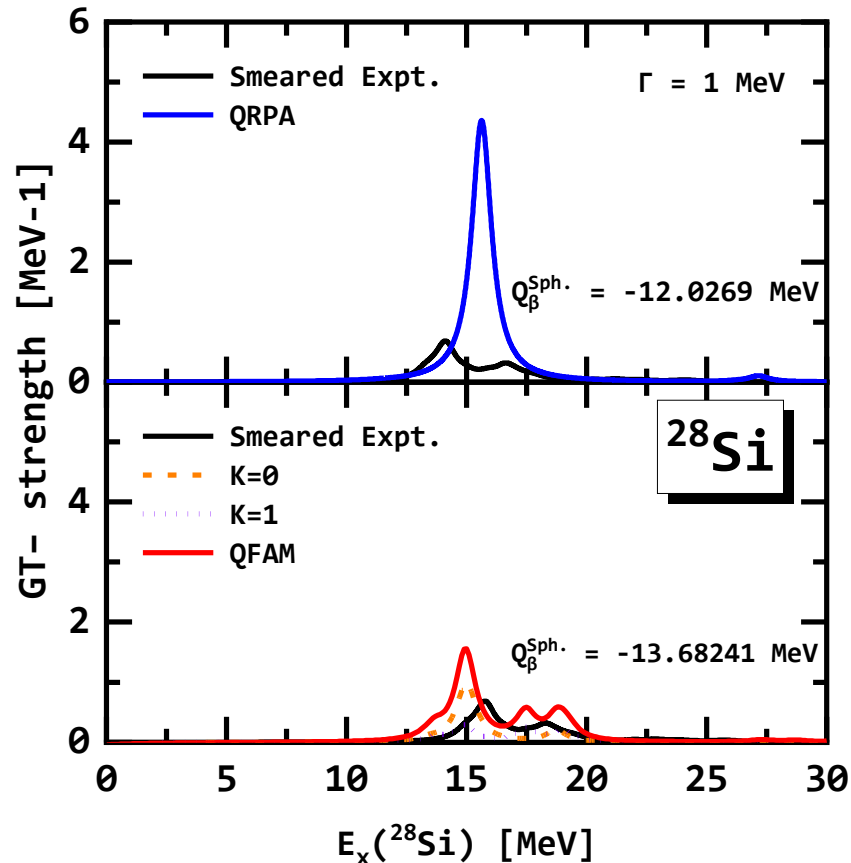
In **spherical** case, E_{GTR} is **overestimated**;

In **deformed** case, E_{GTR} becomes **lower** and **closer to experimental data**;

- The **deformation** leads to the **splitting** in GT- strengths which is closer to the experimental data, although the **splitting** is **too much**.

Preliminary results: Gamow-Teller Transition in ^{24}Mg & ^{28}Si

➤ GT- strengths of ^{28}Si



* $^{28}\text{Si}(p,n)$ from B. D. Anderson et al. Phys. Rev. C 43, 50 (1991).

** Expt. data shift by Q_β to compare with strength related to $E_x(^{24}\text{Mg})$

*** $Q_\beta^{\text{Def.}}$ given by deformed g.s., while $Q_\beta^{\text{Sph.}}$ given by spherical g.s..

- GTR centroid energy: $E_{\text{GTR}} = \frac{\int E_X S dE_X}{\int S dE_X}$;

Z. M. Niu. PhD thesis (2011).

	$E_{\text{GTR}}^{\text{Expt.}}$ [MeV]	$E_{\text{GTR}}^{\text{Theor.}}$ [MeV]	$E_{\text{GTR}}^{\text{Theor.}} - E_{\text{GTR}}^{\text{Expt.}}$ [MeV]
Sph.	15.594	15.613	+0.017
Def.	17.011	16.129	-0.882

In **spherical** case, E_{GTR} is **well reproduced**, but **without splitting**;
 In **deformed** case, E_{GTR} becomes **lower** and **underestimated**.

- The **deformation** leads to the **splitting** in GT- strengths which is closer to the experimental data, but the **1st peak** has **underestimated excitation energy**.

➤ Summary

- We have preliminary developed a **relativistic QFAM** model for **charge-exchange** transitions.
- Nuclear **deformation** leads to the remarkable **splitting** in GT strength;
- Nuclear **deformation** results in a **lower GTR centroid energy** compared to the spherical case.

➤ Outlook

- Completing the QFAM model by including pairing correlation;
- Including the point-coupling functional with tensor coupling and with localized exchanged terms by Fierz transformation PCF-PK1;
-

Thank you!

➤ β_2 -unconstrained calculation: binding energies, deformations & peak energies

